

RESEARCH

Open Access

The effect of film thickness on surface morphology of ITO thin films

Davood Raoufi¹ and Faegh Hosseinpanahi^{1,2*}

Abstract

In this work, we developed the rescaled range method and its formalism to investigate the surface morphology dynamics of indium tin oxide (ITO) thin films. The dynamic scaling behavior of grown ITO thin films, which were prepared by electron beam deposition method on float glass substrates at room temperature, was studied through atomic force microscopy (AFM). AFM data indicated that the average surface roughness values of the films decreased as the film thickness increased from 100 to 250 nm. Based on fractal concept and statistical physics techniques, the irregularities of the ITO films were analyzed. The roughness exponent H and the growth exponent β for ITO films were determined to be 0.71 ± 0.01 and 0.11 ± 0.01 , respectively. The fractal analysis reveals that the value of the fractal dimension D_f ($D_f = 3 - H$) falls within the range 2.29 to 2.24 depending upon the films thickness. These results show that the growth process of the films can be described by the combination of Edwards-Wilkinson and Mullins diffusion models.

Keywords: ITO, Thin film, Fractal analysis, Morphology, Rescaled range analysis (R/S)

PACS: 68.55.Jk, 61.43.Hv

Background

Indium tin oxide (ITO), an n-type semiconductor with a wide band gap (3.5 to 4.3 eV), is of great interest because of its unique features, including high optical transmittance in the visible light wavelength range and high electrical conductivity [1,2]. ITO thin films have been prepared by a variety of methods, such as pulsed laser deposition [3], spray pyrolysis [4], DC and RF magnetron sputtering [5,6], sol-gel process [7], electron beam evaporation [8], and so on. The surface morphology of these prepared ITO directly affects the morphology of organic thin films, because all the organic thin films are deposited on ITO. Thus, the characterization of surface morphology of ITO thin film is one of the most serious problems. Pandey et al. [9] studied the influence of the effect of nickel incorporation on the morphology and the optical and structural properties of electrodeposited diamond-like carbon thin films on ITO-coated glass substrates. Jonda et al. [10] showed the influence of surface roughness on the degradation of OLED by applying

various types of monomeric and polymeric thin films by observing morphological change with AFM. Raoufi and Kalali [11] indicated that the fractal analysis has provided a valuable description of the irregularities in ITO thin film surfaces. In their study, the wavelet coefficients related to the thin film surface profiles have been calculated, and then the roughness exponent (H) of the films has been estimated using the scale gram method. The results reveal that the surface profiles of the films before and after the annealing process have self-affine nature. The understanding of surface growth processes of thin films is a good tool for the investigation of dynamical scaling [12]. In the past decade, many theoretical and experimental efforts were devoted to understand this surface morphology and the dynamics of growing surfaces [13,14]. Thin film growths have fractal characteristic in non-equilibrium situation, which often evolve into self-similarity patterns and well interpreted by a scaling theory [15,16]. The various surface growth mechanisms are proven by different growth models with different sets of scaling exponent. Therefore, the scaling analysis of thin film surface, especially the determining of scaling exponents, can provide an effective way to study the mechanism of surface growth [17]. Thus, for a self-similarity

* Correspondence: F.Hosseinpanahi@yahoo.com

¹Department of Physics, University of Bu Ali Sina, P.O. Box 65174, Hamedan, Iran

²Department of Physics, Payame Noor University, P.O. Box 19395-4697, Tehran, Iran

growing surface, the relationship between the interface width and various scaling exponents can be described by the dynamic scaling form, wherein the height fluctuation over a length scale is studied:

$$w(L, t) = L^H f\left(tL^{-\frac{H}{\beta}}\right) \quad (1)$$

where w is the roughness of the surface on length scale L at time t . H and β are the Hurst exponent (roughness exponent) and the growth exponent, respectively [18,19]. The most usual records of observable quantities are in the form of ordered sequences (e.g., time series), fluctuations perpendicular to the surface, and their fractal properties which have been extensively investigated [20]. With this purpose, many methods have been proposed, such as rescaled range analysis (R/S) [21], height-different correlation function, [22] etc. R/S has been recently used extensively in the image and signal processing as a new method. R/S has the advantage of fast computation with localization in space domains and is well adapted in the analysis of surface roughness, providing an insight into the stochastic properties of a fractal surface. In this study, we employ atomic force microscopy (AFM) to investigate the surface morphology parameters of ITO films using the scaling theory. AFM images of the evaporated deposition ITO films indicate changes in the surface behavior of the films at different thicknesses.

Experimental procedure

ITO thin films, with different thicknesses ranging from 100 to 250 nm, were prepared by electron beam evaporation method on polished float (soda-lime) glass substrates at room temperature. The target material used in this study was an ITO pellet (Merck Sharp & Dohme Corp., NJ, USA) with nominal 99.9% purity $\text{In}_2\text{O}_3\text{:SnO}_2$ (90 and 10 wt%, respectively). Before loading the glass substrates into the chamber, they were ultrasonically cleaned in acetone, ethanol, and deionized water for 10 min. Finally, they were dried with nitrogen gas. The optimum conditions of the films deposited were achieved in the presence of oxygen with an initial vacuum (base pressure) of 1×10^{-6} mbar, an accelerating voltage of 1 to 10 kV, and an electron beam current of 10 to 12 mA. For controlling the deposition rate, the oxygen (99.99%) is introduced into the deposition system from a steel tube through a calibrated leak valve. Using the data from a quartz crystal thickness measurement system, the electron gun current is automatically adjusted to have a constant deposition rate. The deposition rate was 0.1 nm s^{-1} and the thickness of the ITO thin films varied in the range of 100 to 250 nm. After preparing the films, each sample was taken out for immediately *ex situ* measurements to study the surface

morphology of the films. The surface morphology of the thin films was characterized with an atomic force microscope (Park Scientific Instruments, CA, USA) under ambient conditions. The scan size was $1 \times 1 \mu\text{m}^2$. All the surface images were obtained in the contact mode using silicon nitride tips with approximate tip radius of 10 nm, and the height of the surface relief was recorded at a resolution of 256×256 pixels. A variety of scans were acquired at random locations on the film surface. To analyze the AFM images, the topographic image data were converted into ASCII data.

Rescaled range analysis

The classic R/S analysis or Hurst exponent on a discrete time series was used as a tool to describe the self-similarity parameters. This method was used to study the statistical characteristics of the fractal signals [23-26]. In this procedure, it is necessary to introduce a time series of length N . We divide them into M adjacent subinterval of length L , while $M \times L = N$. Each subinterval is labeled by I_a , with $a = 1, 2, \dots, M$; each element in I_a is labeled by $N_{k,a}$, such that $k = 1, 2 \dots L$. For each subinterval in the time series, the following procedure was used:

The average and standard deviation are calculated as:

$$M_a = \frac{1}{L} \sum_{i=1}^L N_{k,a} \quad (2)$$

$$S_{I_a} = \sqrt{\frac{1}{L} \sum_{k=1}^L [N_{k,a} - M_a]^2} \quad (3)$$

We compute $X_{k,a}$, that is, the time series of accumulated departures from the mean for each subinterval I_a , which is defined as:

$$X_{k,a} = \sum_{i=1}^k [N_{i,a} - M_a] \quad k = 1, 2, \dots, L \quad (4)$$

The range (R_{I_a}) that is the difference between the maximum and the minimum values of the subinterval I_a is defined as:

$$R_{I_a} = \max(X_{k,a}) - \min(X_{k,a}) \quad (5)$$

Rescaling the range $\left(\frac{R_{I_a}}{S_{I_a}}\right)$ of each subinterval computed by dividing the standard deviation and then calculating the average of rescaled range for all subintervals of length L :

$$\left(\frac{R}{S}\right)_L = \frac{1}{M} \sum_{a=1}^M \left(\frac{R_{I_a}}{S_{I_a}}\right) \quad (6)$$

The length of L must be increased, and the whole process is repeated until $L = N / 2$. Finally, we plotted

the logarithm of $(R / S)_L$ vs. the logarithm of L as the dependent variable and the independent variable, respectively. The slope of this plot is the estimate of the H , where H is the Hurst exponent [21].

$$\left(\frac{R}{S}\right)_L = \text{const} \times L^H \quad (7)$$

Edwards-Wilkinson and Mullins diffusion equations

Edwards-Wilkinson equation

A simple growth model is investigated, where particles are deposited onto a substrate randomly and subsequently relaxed into a position nearby where the binding is strongest. Kinetic roughening has attracted a lot of attention over the last few years not only because of its practical importance for the growth of solid films, but also because it sets as an example for a dynamical mechanism that drives a system into a spatially and temporally scale invariant state (self-organized criticality) [27,28]. Most of the models of kinetic roughening studied so far can be described by the Edwards-Wilkinson (EW) equation [29]:

$$\frac{\partial h(x, t)}{\partial t} = v\nabla^2 h(x, t) + \eta(x, t) \quad (8)$$

where $h(x, t)$ is the height of the surface at time t above the substrate site specified; v has a smoothening effect on the surface, while the white noise $\eta(x, t)$ due to fluctuations in the growth rate makes the surface rough. In this model, the particle moves to the lowest surface site in the neighborhood instead to the one of maximum number of bonds. The Laplacian term in the EW equation is referred to as the surface relaxation term, because the effect of the Laplacian is to smoothen the surface profile while keeping the mean height unchanged.

Mullins diffusion equation

To model the surface diffusion in a stochastic continuum equation, consider a macroscopic current of particles on the surface, represented by the vector $j(x, t)$. Because diffusion conserves the total number of particles on the surface, $j(x, t)$ must satisfy the continuity relation [30]:

$$\frac{\partial h(x, t)}{\partial t} = -\nabla \cdot j(x, t) \quad (9)$$

In addition, the surface current $j(x, t)$ is related to the gradient of the chemical potential, $j(x, t) \propto -\nabla \mu(x, t)$, because the surface current will flow from areas of higher potential to areas of lower potential. Also, the chemical potential $\mu(x, t)$ is related to the number of bonds that must be broken by an atom to diffuse. Regions of the surface which have a positive curvature have

more available bonds, which in turn makes it harder for an atom to diffuse. Conversely, regions of the surface with negative curvature have fewer available bonds, and an atom can diffuse more readily. These conditions are satisfied if $\mu(x, t) \propto -\nabla^2 h(x, t)$. Combining these results,

$$\frac{\partial h(x, t)}{\partial t} = -\nabla \cdot [-\nabla (-k\nabla^2 h(x, t))] = -k\nabla^4 h(x, t) \quad (10)$$

This suggests adding a bi-harmonic term to the growth equation to model surface diffusion

$$\frac{\partial h(x, t)}{\partial t} = -k\nabla^4 h(x, t) + \eta(x, t) \quad (11)$$

which is known as the Mullins diffusion equation [31,32]. These models are able to predict values for the exponents H and β analytically. The exponent H , called the Hurst (roughness) exponent, is a critical exponent that characterizes the roughness of saturated interface; the exponent β , which is called the growth exponent, characterizes the time-dependent dynamics of the roughening process.

Results and discussions

Evolution features of the ITO thin films

In order to analyze the AFM images, the height (z scale) of each point of the AFM data (here, a matrix of 256×256 pixels) was converted into ASCII data as a linear matrix ($1 \times 65,536$). This series (linear matrix) is used in R/S model, and it is necessary to introduce a time series of length N .

Figure 1a,b,c shows the AFM images of the ITO thin films deposited on a glass substrate over the scan area of $1 \times 1 \mu\text{m}^2$. From these images, it is clear that the ITO thin film surfaces show continuous island-like structures, and with increasing film thickness, these islands become smaller in both lateral and vertical directions.

The surface of the 100-nm film is highly rough, with an average roughness (R_a) of 19.8 nm and an interface width w (RMS) roughness 24.8 nm. The average roughness is defined as the average value of the absolute distances of the surface points from the mean plane, while the interface width w (RMS) roughness is the standard deviation of the surface from the mean plane within the sampling area [33].

The evolution feature can be more easily observed from the corresponding surface profiles (insets) of these films in Figure 2. From this figure, it is noted that the interface width w (RMS) values are decreased with increasing film thickness. These results are consistent with those of Shigesato et al.'s [34] work, where the R_a of the ITO/glass remarkably changes with increasing thickness,

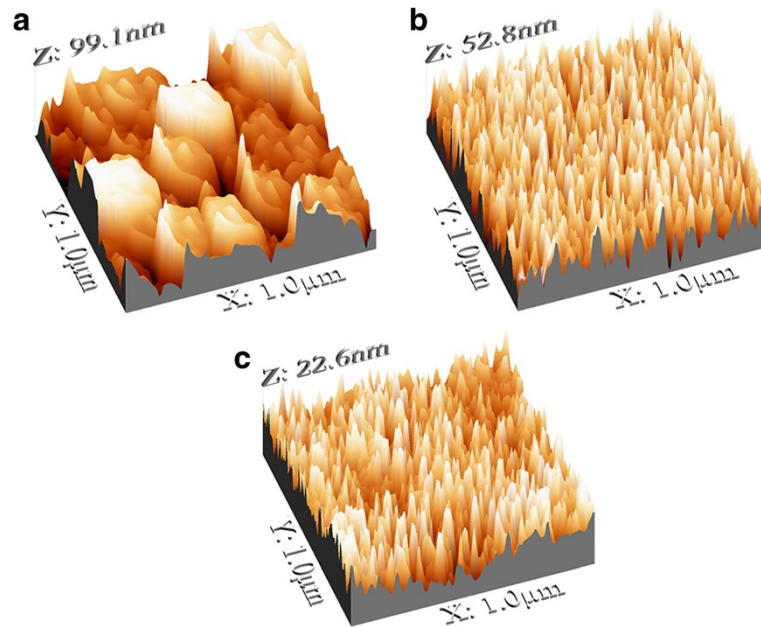


Figure 1 An AFM image series of the ITO thin films. (a) 100 nm, (b) 150 nm, and (c) 250 nm.

reflecting nucleation, coalescence, and continuous film growth processes, i.e., Volmer-Weber-type initial growth.

Atomic force microscopic analysis is ideal to quantitatively measure the nanometric dimensional surface roughness and for visualizing the surface texture of the

deposited film. The surface texture of the ITO thin films, with horizontal length scale of 1 micron, is represented in Figure 3a,b,c. The statistical analysis of the AFM data was done using the height distribution histograms (Figure 3). To calculate the measure of asymmetry

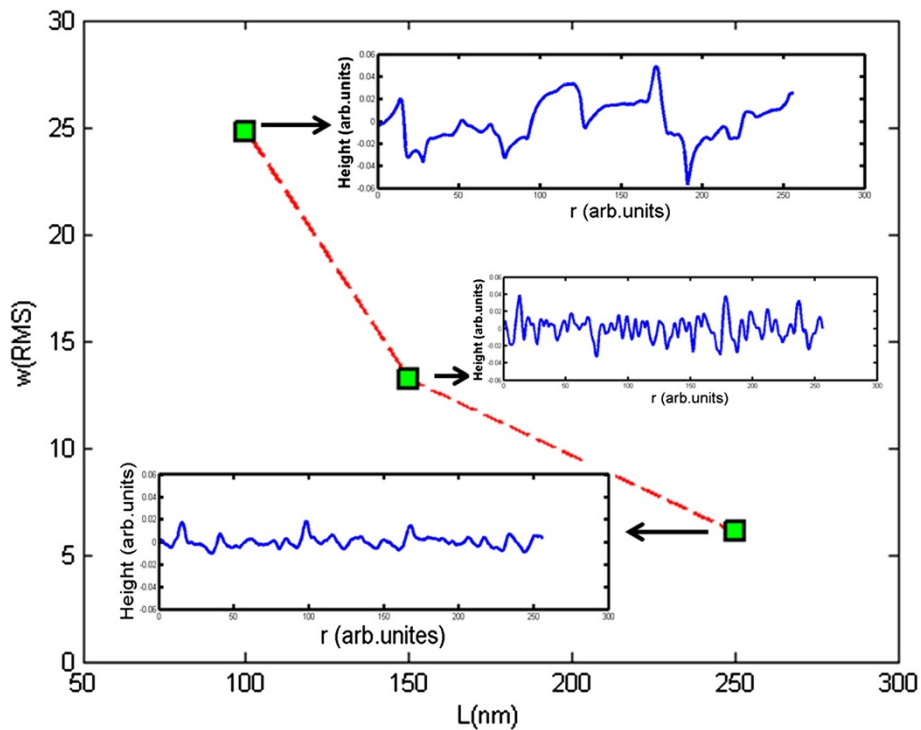


Figure 2 Relationship between w (RMS) and profile scan of Figure 1.

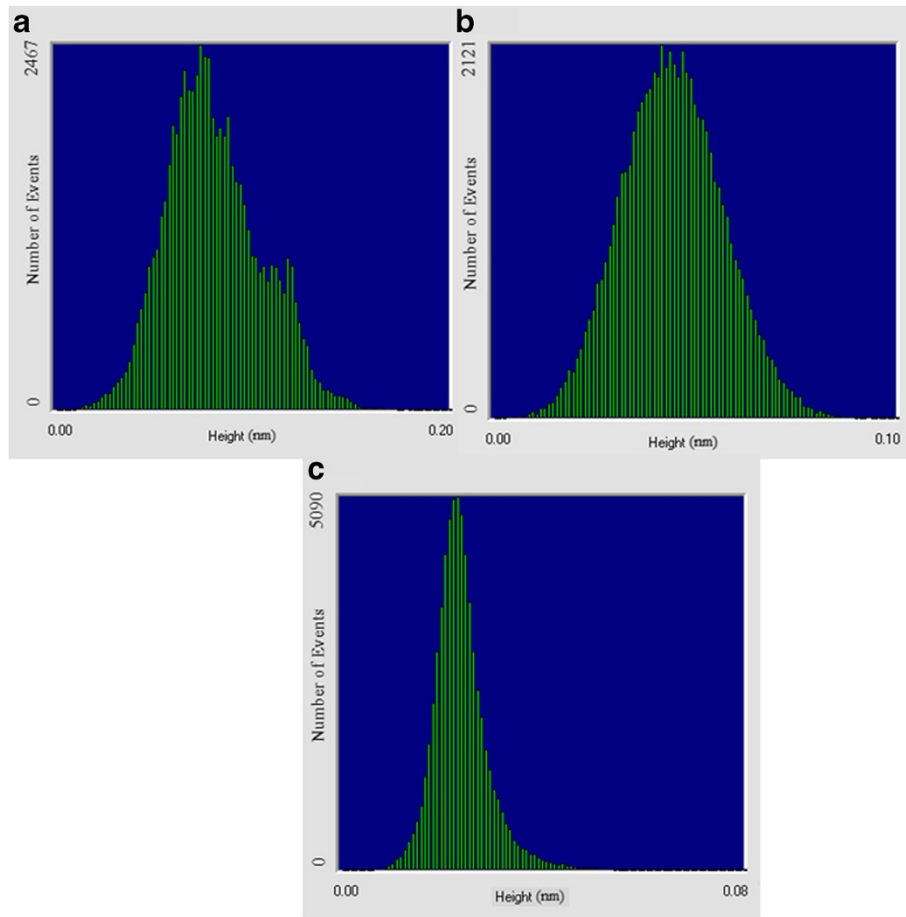


Figure 3 (a-c) height distribution from the AFM images (Figure 1). This figure estimated from the AFM images of figure 1 (a-c).

of the height distribution surface, we used statistical parameters surface skewness and kurtosis [35]. The skewness and kurtosis are the third and fourth moments of the distribution function, respectively. For the Gaussian distribution, the skewness and the kurtosis are equal to zero and three, respectively. Denoting $h(i, j)$ as the height of the surface measured by AFM at the point (i, j) and $N \times N$ as the total number of points at which the surface heights have been measured, the skewness and kurtosis were defined using the equation:

$$R_{sk} = \frac{1}{w^3} \langle [h(i, j) - \langle h(i, j) \rangle]^3 \rangle \quad (12)$$

$$R_{ku} = \frac{1}{w^4} \langle [h(i, j) - \langle h(i, j) \rangle]^4 \rangle \quad (13)$$

where $\langle h(i, j) \rangle$ is the mean value of heights of the surface, and w is the root mean square roughness and is defined as below [24]:

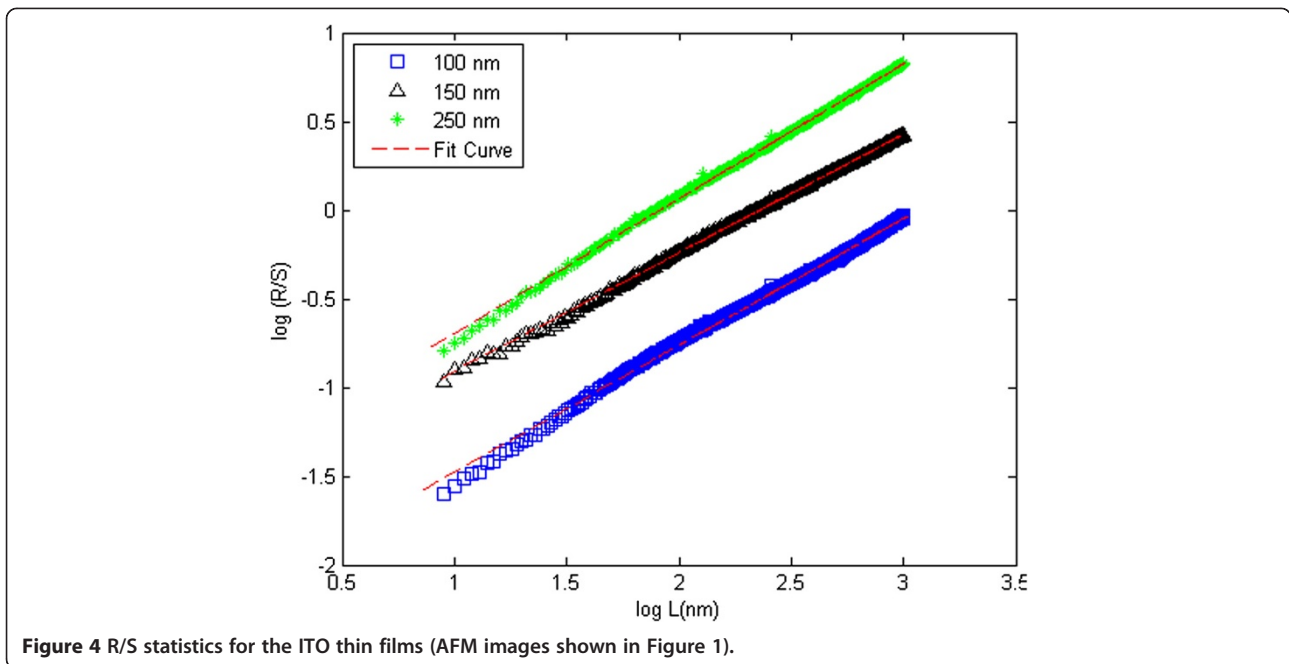
$$w = \frac{1}{N} \sqrt{\sum_{i=j=1}^N (h(i, j) - \langle h(i, j) \rangle)^2} \quad (14)$$

In the case of $R_{ku} > 3$, the surface has relatively less high peaks and low valleys, while bumpy surfaces possess lower values. On the other hand, $R_{ku} < 3$ shows more high peaks and low valleys over the surface [36].

Film surfaces with positive skewness ($R_{sk} > 0.2$) and high kurtosis ($R_{ku} > 3$) values are suitable for tribological applications (e.g., low-friction bearings) [37]. In the present study, all the thin films investigated are close to these criteria (see Table 1); hence, ITO is a potential material suitable for tribological applications.

Table 1 Statistical parameters of ITO thin films in relation to films thickness

Sample	Thickness (nm)	R_a (nm)	w (nm)	R_{sk}	R_{ku}	H
a	100	19.8	24.8	0.37	3.04	0.71 ± 0.01
b	150	10.5	13.2	0.14	3.03	0.67 ± 0.01
c	250	4.51	6.09	1.40	8.59	0.76 ± 0.01

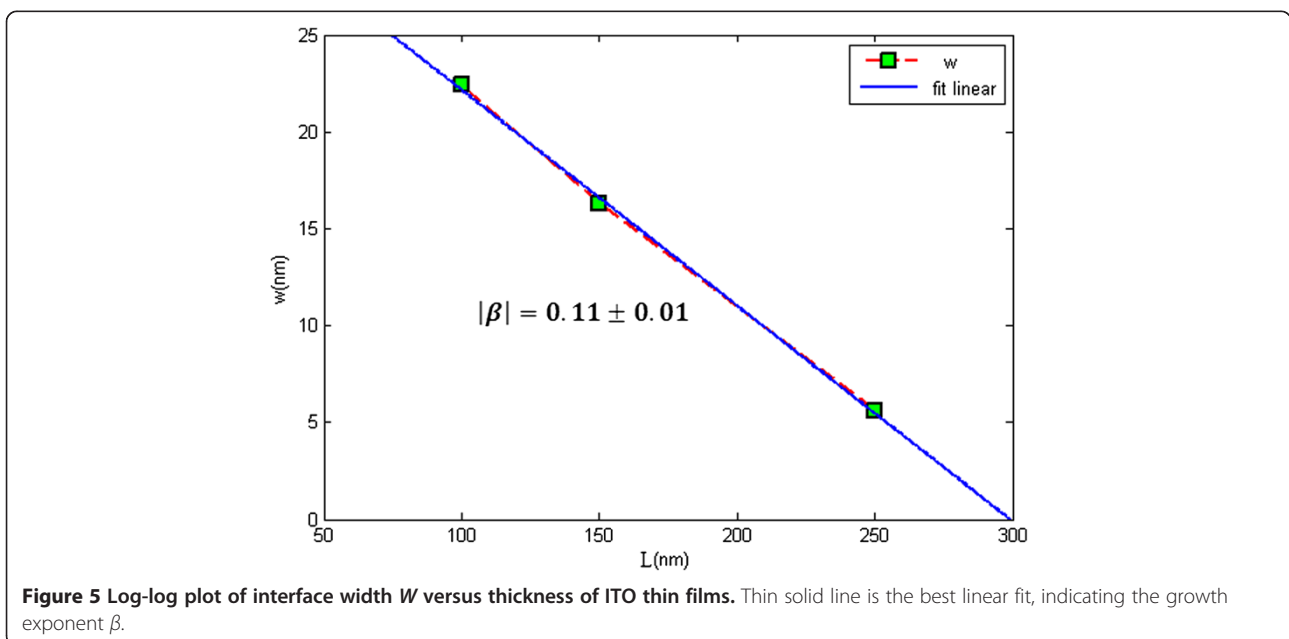


The films were estimated from the AFM images (Figure 1).

The above analyses indicate that statistical parameters are strongly affected by the degree of aggregation and cluster size of the films. The different cluster sizes influence the surface roughness of the films [38]. However, these statistical measurements are given only with height information, and rather inadequate to provide a complete description of the irregularity of thin film surfaces, therefore cannot fully characterize the surface.

Scaling behavior of the ITO thin films

The Hurst exponent has been used for the measured self-similarity parameters and for the investigation of the correlations at long-range dependence in empirical time series. The H was seen to be between 0 and 1. The value $H = 0.5$ indicates that the time series is independent, e.g., the process probably be a non-Gaussian. However, the estimates for pure Gaussian distribution process can strongly deviate from the limit of $H = 0.5$. $H > 0.5$ indicates that the time series is persistence, and $H < 0.5$



means anti-persistence or pure random character of records [39,40]. Thus, these behaviors are the bases of non-linear dynamics in the system. The Hurst exponent is directly related to the fractal dimension (D_f) of the random surface by $D_f = [(E + 1) - H]$, where $E + 1$ is the dimension of the embedded space ($E = 1$ for a profile; $E = 2$ for a plan) [41,42]. The fractal dimension corresponds to the changes in the surface morphology. A larger value of fractal dimension corresponds to more jagged morphology, while a smaller one corresponds to a locally smooth surface structure. The fractal analysis reveals that the value of the fractal dimension ($D_f = 3 - H$) falls within the range 2.29 to 2.24, depending upon the films thickness.

Figure 4 presents the rescaled range analysis for ITO thin films prepared on glass slide substrates at room temperature, by electron beam evaporation technique. From this graph, the H value was obtained by means of a statistical regression as the slope of the straight line. The slopes of the curves represent the Hurst exponent ranging from 0.71 ± 0.01 to 0.76 ± 0.01 , which characterize the time series structure (see Table 1). The value of H that is greater than 0.5 indicates that it is persistent, i.e., long memory; that means that there are extended periods in which the system deviates from the long term mean. Two features are recognized by looking at Figure 4. The first feature is the tendency of plot R/S to shift up (corresponding to a smaller value of RMS roughness w) as the film thickness increases. The second feature is the Hurst exponent having an average value of 0.71 ± 0.01 , showing that the Hurst coefficient did not change substantially with the increase in thickness, i.e., the Hurst exponent for all samples are very close. This suggests that the dynamics of roughness formation may be quite similar during the increase of the thickness of the ITO thin films [43]. We compare the average H and β values determined for ITO thin films with their exponents to suggest the theoretical models combining the smoothing mechanism with random fluctuations; one can describe the growth process by a Langevin equation in the form:

$$\frac{\partial h(x, t)}{\partial t} = v \nabla^2 h(x, t) - k \nabla^4 h(x, t) + \eta(x, t) \quad (15)$$

where $v \nabla^2 h(x, t)$ is the result of the Gibbs-Thompson relation describing the thermal equilibrium interface between the vapor and solid. The term $\nabla^2 h(x, t)$ is the small slope expansion of the surface curvature, and the pre-factor $v \nabla^2 h(x, t)$ is proportional to the surface tension coefficient. The second term $-k \nabla^4 h(x, t)$ is the result of surface diffusion due to the curvature-induced chemical potential gradient. The pre-factor k is proportional to the surface diffusion coefficient. We can see

that the general Langevin equation is a combination of the EW and Mullins diffusion equations. Therefore, the $0 \leq \beta \leq 0.25$ value is between the EW model, $\beta = 0$, and the Mullins diffusion model, $\beta = 0.25$ [44]. Figure 5 describes the dependence of the interface width W on thickness L for different ITO thin films. The thin solid line is the best linear fit indicating β , and the result of the fit gives $\beta = 0.11 \pm 0.01$.

From the above analysis, $H = 0.71 \pm 0.01$ and $\beta = 0.11 \pm 0.01$. From the measured Hurst exponent and growth exponent, we suggest that our ITO thin film growth behavior is the result of the combined Mullins diffusion model and the Edwards-Wilkinson model.

Conclusions

The surface morphologies of the ITO thin films, prepared by electron beam deposition method, at different films thickness were measured by AFM. A statistical analysis of the ITO thin films has been performed based on R/S method. The statistical analysis of the AFM data showed that the relatively high kurtosis, positive skewness, and minimum roughness of the films increased with the increase of the film thickness from 100 to 250 nm. Our analyses have also revealed that the growth process of the ITO thin films can be described by the combination of Edwards-Wilkinson and Mullins diffusion models.

Competing interests

The authors declare that they have no competing interests.

Authors' contributions

DR made the ITO thin films and conceived of the study. FH participated in the design of the study, performed the statistical analysis, and drafted the manuscript. Both authors read and approved the final manuscript.

Acknowledgments

The authors would like to thank Dr. G.R. Jafari from the Department of Physics, Shahid Beheshti University, for the many useful discussions and for helping in the R/S analysis of the films.

Received: 13 August 2012 Accepted: 17 March 2013

Published: 10 May 2013

References

1. Djuricic, AB, Kwong, CY, Chui, PC, Chan, WK: Indium-tin-oxide surface treatments: Influence on the performance of CuPc/C₆₀ solar cells. *J. Appl. Phys* **93**, 5472–5479 (2003)
2. Kim, H, Pique, A, Horwitz, JS, Mattoussi, H, Murata, H, Kafafi, ZH, Chrisey, DB: Indium tin oxide thin films for organic light-emitting devices. *Appl. Phys. Lett* **74**, 3444–3446 (1999)
3. Yong, T-K, Tan, S-S, Nee, C-H, Yap, S-S, Kee, Y-Y, Sáfrán, G, Horvath, ZE, Moscatello, J, Yap, Y-K, Tou, T-Y: Pulsed laser deposition of indium tin oxide nanowires in argon and helium. *Mater. Lett* **66**, 280–282 (2012)
4. El Rhaleb, H, Benamar, E, Rami, M, Roger, JP, Hakam, A, Ennaoui, A: Spectroscopic ellipsometry studies of index profile of indium tin oxide films prepared by spray pyrolysis. *Appl. Surf. Sci* **201**, 138–145 (2002)
5. Deng, W, Ohgi, T, Nejo, H, Fujita, D: Development of conductive transparent indium tin oxide (ITO) thin films deposited by direct current (DC) magnetron sputtering for photon-STM applications. *Appl. Phys. A: Mater. Sci. Process* **72**, 595–601 (2001)

6. Hu, YL, Diao, XG, Wang, C, Hao, WC, Wang, TM: Effects of heat treatment on properties of ITO films prepared by rf magnetron sputtering. *Vacuum* **75**, 183–188 (2004)
7. Kim, SS, Choi, SY, Park, CG, Jin, HW: Transparent conductive ITO thin films through the sol-gel process using metal salts. *Thin Solid Films* **347**(1–2), 155–160 (1999)
8. Fallah, HR, Ghasemi, M, Hassanzadeh, A, Steki, H: The effect of annealing on structural, electrical and optical properties of nanostructured ITO films prepared by e-beam evaporation. *Mater. Res. Bull.* **42**, 487–496 (2007)
9. Pandey, B, Pal, PP, Bera, S, Ray, SK, Kar, AK: Effect of nickel incorporation on microstructural and optical properties of electrodeposited diamond like carbon (DLC) thin films. *Appl. Surf. Sci.* **261**, 789–799 (2012)
10. Jonda, C, Mayer, ABR, Stolz, U, Elschner, A, Karbach, A: Surface roughness effects and their influence on the degradation of organic light emitting devices. *Mater. Sci.* **35**, 5645–5651 (2000)
11. Raoufi, D, Kalali, Z: Wavelet-fractal approach to surface characterization of nanocrystalline ITO thin films. *Physica B* **407**, 4369–4374 (2012)
12. Kardar, M, Parisi, G, Zhang, Y-C: Dynamic scaling of growing interfaces. *Phys. Rev. Lett.* **56**, 889–892 (1986)
13. Barabasi, AL, Stanley, H: *Fractal Concepts in Surface Growth*. Cambridge University Press, Cambridge, England (1995)
14. Meakin, P: *Fractals, Scaling and Growth Far from Equilibrium*. Cambridge University Press, Cambridge, UK (1998)
15. Family, F, Vicsek, T: *Dynamics of Fractal Surfaces*. World Scientific, Singapore (1991)
16. Family, F, Vicsek, T: Scaling of the active zone in the Eden process on percolation networks and the ballistic deposition model. *J. Phys. A* **18**, L75 (1985)
17. Chu, K, Liu, Z-J, Lu, YH, Shen, YG: Atomic force microscopy study of growth kinetics: scaling in TiN–TiB₂ nanocomposite films on Si(100). *Appl. Surf. Sci.* **252**, 8091–8095 (2006)
18. Tang, LH, Forrest, BM, Wolf, DE: Kinetic surface roughening. II. Hypercube-stacking models. *Phys. Rev. A* **45**, 7162–7179 (1992)
19. Amar, JG, Family, F: Numerical solution of a continuum equation for interface growth in 2 + 1 dimensions. *Phys. Rev. A* **41**, 3399–3402 (1990)
20. Raoufi, D: Fractal analyses of ITO thin films: a study based on power spectral density. *Physica B* **405**, 451–455 (2010)
21. Hurst, HE, Black, RP, Simaika, YM: *Long-Term Storage: An Experimental Study*. Constable, London (1965)
22. Singh, S, Basu, S: Structure and morphology of the Ni films grown by different deposition methods. *Surf. Coat. Tech.* **201**, 952–957 (2006)
23. Jones, CL, Lonergan, GT, Mainwaring, DE: Wavelet packet computation of the Hurst exponent. *J. Phys. A* **29**, 2509–2527 (1996)
24. Heneghan, C, McDarby, G: Establishing the relation between detrended fluctuation analysis and power spectral density analysis for stochastic processes. *Phys. Rev. E* **62**, 6103–6110 (2000)
25. Lung, CW, Jiang, J, Tian, EK, Zhang, CH: The relation between fractal dimension and roughness index for fractal surface. *Phys. Rev. E* **60**, 5121–5130 (1999)
26. Carreras, BA, van Milligen, BPH, Pedrosa, MA, Balbin, R, Hidalgo, C, Newman, DE, Sanchez, E, Frances, M, Garcia-Cortes, I, Bleuel, J, Endler, M, Ricardi, C, Davies, S, Matthews, GF, Martinez, E, Antoni, V, Latten, A, Klinger, T: Self-similarity of the plasma edge fluctuations. *Phys. Plasmas* **5**, 3632–3642 (1998)
27. Wolf, DE, Villain, J: Growth with surface diffusion. *Europhys. Lett.* **13**, 389–394 (1990)
28. Krug, J, Spohn, H: Growth and aggregation far from equilibrium. In: Godreche, C (ed.) *Solids Far from Equilibrium: Growth, Morphology and Defects*, pp. 433–460. Cambridge University Press, Cambridge (1990)
29. Edwards, SF, Wilkinson, DR: The surface statistics of a granular aggregate. *Proc. R. Soc. London Ser. A* **381**, 17–31 (1982)
30. Pelliccione, M, Toh-Ming, L: *Evolution of Thin Film Morphology: Modeling and Simulations*. Springer, New York (2007)
31. Das Sarma, S, Tamborenea, P: A new universality class for kinetic growth: one-dimensional molecular-beam epitaxy. *Phys. Rev. Lett.* **66**, 325–328 (1991)
32. Mullins, WW: Theory of thermal grooving. *J. Appl. Phys.* **28**, 333–340 (1957)
33. Tudose, IV, Horvath, P, Sucheai, M, Christoulakis, S, Kitsopoulos, T, Kiriakidis, G: Correlation of ZnO thin film surface properties with conductivity. *J. Appl. Phys.* **89**, 57–62 (2007)
34. Shigesato, Y, Koshi-ishi, R, Kawashima, T, Ohsako, J: Early stages of ITO deposition on glass or polymer substrates. *Vacuum* **59**, 614–621 (2000)
35. Jason, T, Dorta, YP, Lu, Zhao, TM, Wang, GC: Numerical of the noisy Kuramoto-Sivashinsky equation in 2 + 1 dimension. *Phys. Rev. E* **59**, 177–185 (1999)
36. Wang, W-Z, Chen, H, Hu, Y-Z, Wang, H: Effect of surface roughness parameters on mixed lubrication characteristics. *Tribol. Int.* **39**, 522–527 (2006)
37. Daniel, GP, Justinvictor, VB, Naira, PB, Joy, K, Koshy, P, Thomas, PV: Effect of annealing temperature on the structural and optical properties of ZnO thin films prepared by RF magnetron sputtering. *Physica B* **405**, 1782–1786 (2010)
38. Buzio, R, Gnecco, E, Boragno, C, Valbusa, U, Piseri, P, Barborini, E, Milani, P: Self-affine properties of cluster-assembled carbon thin films. *Surf. Sci.* **444**, L1–L6 (2000)
39. Norouzzadeh, P, Jafari, GR: Application of multifractal measures to Tehran price index. *Physica A* **356**, 609–627 (2005)
40. Carvalho, LMV, Tsonis, AA, Jones, C, Rocha, HR, Polito, PS: Anti-persistence in the global temperature anomaly field. *Nonlin. Processes Geophys.* **14**, 723–733 (2007)
41. Ioannou-Sougleridis, V, Constantoudisa, V, Alexeb, M, Scholz, R, Vellianitisc, G, Dimoulas, A: Effects on surface morphology of epitaxial Y₂O₃ layers on Si (100) after post growth annealing. *Thin Solid Films* **468**, 303–309 (2004)
42. Qi, HJ, Huang, LH, Yuan, JM, Cheng, CF, Shao, JD, Fan, ZX: Dynamic scaling in growth of ZrO₂ thin films prepared by electronic beam evaporation. *Chin. Phys. Lett.* **20**, 709–712 (2003)
43. Raoufi, D, Kiasatpour, A, Fallah, HR, Rozatian, ASH: Surface characterization and microstructure of ITO thin films at different annealing temperatures. *Appl. Surf. Sci.* **253**, 9085–9090 (2007)
44. Zhao, Y, Ching, G, Wang, Ming Lu, T: *Characterization of Amorphous and Crystalline Rough Surface: Principle and Applications*. Academic, New York (2001)

doi:10.1186/2251-7235-7-21

Cite this article as: Raoufi and Hosseinpanahi: The effect of film thickness on surface morphology of ITO thin films. *Journal of Theoretical and Applied Physics* 2013 7:21.

Submit your manuscript to a SpringerOpen[®] journal and benefit from:

- Convenient online submission
- Rigorous peer review
- Immediate publication on acceptance
- Open access: articles freely available online
- High visibility within the field
- Retaining the copyright to your article

Submit your next manuscript at ► springeropen.com